ISSN 1063-7834, Physics of the Solid State, 2020, Vol. 62, No. 2, pp. 297–307. © Pleiades Publishing, Ltd., 2020.
Russian Text © The Author(s), 2020, published in Fizika Tverdogo Tela, 2020, Vol. 62, No. 2, pp. 247–256.

MAGNETISM

Physical Properties of a Frustrated Quasi-One-Dimensional $NaCuFe_2(VO_4)_3$ Magnet and Effect of Chemical Pressure Induced by the Substitution of Sodium for Lithium

T. V. Drokina[a, *], G. A. Petrakovskii[a], O. A. Bayukov[a], M. S. Molokeev[a, b], A. M. Vorotynov[a], S. I. Popkov[a, b], and D. A. Velikanov[a]

[a] *Kirensky Institute of Physics, Krasnoyarsk Scientific Center, Siberian Branch, Russian Academy of Sciences, Krasnoyarsk, 660036 Russia*

[b] *Siberian Federal University, Krasnoyarsk, 660041 Russia*

**e-mail: tvd@iph.krasn.ru*

Received September 24, 2019; revised September 24, 2019; accepted September 24, 2019

Abstract—The structural, thermal, static magnetic, and resonance properties of the low-dimensional $NaCuFe_2(VO_4)_3$ compound obtained by the solid-phase synthesis have been investigated. In the temperature range of 110–300 K, the electron spin resonance in the X band with a *g* factor of 2.008 has been detected. The magnetic properties of a sample with a high frustration level in the paramagnetic, antiferromagnetic, and disordered states have been examined. A shift of the Néel temperature to the high-temperature region in an external magnetic field has been observed. The origin of the disordered magnetism in $NaCuFe_2(VO_4)_3$ are discussed. The features of substitution of sodium for lithium on the physical properties of the $ACuFe_2(VO_4)_3$ (A = Na, Li) system have been established. It is shown that the chemical pressure changes the crystal lattice parameters, spacings between magnetic ions, and crystallite size, which is reflected in the physical properties of the material.

Keywords: multicomponent vanadates, structural features, magnetic properties, phase transitions, chemical pressure

DOI: 10.1134/S1063783420020122

1. INTRODUCTION

The synthesis and study of the complex oxide compounds containing 3*d* transition metals, including multicomponent vanadates, have been in focus of researchers in the field of condensed matter physics due to the features of their crystal structure, which allows the competition of magnetic interactions leading to the frustration of magnetic moments [1–4]. The frustrated magnetic systems with their diverse magnetic structures (in particular, complex spirals with helicoid and cycloid elements) and transitions between them have unique properties, which are caused by the ground state energy degeneracy and high sensitivity to various perturbations [5–10].

It is well known that the properties of condensed systems can change not only under the action of external factors (e.g., temperature, magnetic and electric fields, and pressure), but also under the chemical pressure induced by cationic or anionic substitutions. Study of the effect of external factors and chemical pressure on the properties of materials remains an urgent problem of modern physics, which opens up prospects for new applications.

According to the literature data on the properties of vanadates with the general formula $ACuFe_2(VO_4)_3$ (A is a univalent alkali metal), the howardevansite $NaCuFe_2(VO_4)_3$ was discovered in the eighties of the twentieth century among the minerals found near the Isalco volcano in El Salvador and the composition and crystal structure of the natural material were studied first in [11].

The structure of the synthesized $LiCuFe_2(VO_4)_3$ compound was determined in [12]. The results of investigations of the structural, static magnetic, and resonance properties of the $LiCuFe_2(VO_4)_3$ magnet obtained by the solid-state synthesis were reported in [4]. At low temperatures, a long-range magnetic order was found in the magnetic subsystem of the sample, which has a chain spin structure with the predominantly antiferromagnetic exchange coupling and a high frustration level. The parameters of exchange interactions in the six-sublattice magnet representation were estimated using the indirect coupling model. It was shown that $LiCuFe_2(VO_4)_3$ is an antiferromagnet with the strong intrachain and frustrating interchain exchange interactions.

The magnetodielectric effect in $LiCuFe_2(VO_4)_3$ was reported in [13]; it was found that an external magnetic field causes the growth of its permittivity.

The electrical properties of the $LiCuFe_2(VO_4)_3$ and $NaCuFe_2(VO_4)_3$ compounds as functions of frequency and temperature were studied in [14, 15]. In [15], the impedance spectroscopy investigations in the frequency range from 300 Hz to 5 MHz at temperatures of 523–673 K revealed signals from the phases of both bulk grains and grain boundaries of a polycrystalline material. The latter was not found in the compound with lithium [14]. The authors concluded that electric transport is caused by the motion of Na^+ (Li^+) cations along the [001] channel and the $LiCuFe_2(VO_4)_3$ compound is a better conductor than $NaCuFe_2(VO_4)_3$.

The $ACuFe_2(VO_4)_3$ (A = Na, Li) compounds with a number of features, including the quasi-one-dimensional magnetic subsystem and competing magnetic interactions, have attracted attention of researchers [2] who studied the electrical and magnetic properties and relation between them. The authors reported the transformation of a magnetic subsystem in the $ACuFe_2(VO_4)_3$ compounds at two critical temperatures and reported the results of investigations of the dielectric properties of materials confirming the properties of a multiferroic in the $LiCuFe_2(VO_4)_3$ vanadate.

In this work, we extend the investigations of the properties of the multicomponent $NaCuFe_2(VO_4)_3$ vanadate and report the results of X-ray structural, thermal, magnetic, and resonance studies. In the paramagnetic region in the X band, the electron spin resonance was observed, which has a g factor of 2.008. The effect of a magnetic field on the temperature of the phase transition from the paramagnetic to magnetically ordered state was established. The origin of the disordered magnetism in $NaCuFe_2(VO_4)_3$ is discussed. To examine the effect of the chemical pressure induced by the cationic substitution, the properties of the $ACuFe_2(VO_4)_3$ (A = Na, Li) oxides were compared.

2. EXPERIMENTAL

The $NaCuFe_2(VO_4)_3$ samples were obtained by the solid-state synthesis. The charge used was a mixture of the Fe_2O_3, Na_2CO_3, CuO, and V_2O_5 oxides taken in the stoichiometric ratio. Tablets prepared from the charge were annealed in air at temperatures of 650 and 680°C for 24 h. The $LiCuFe_2(VO_4)_3$ synthesis conditions used in this study were described in [4]. The chemical and phase compositions of the samples were explored by X-ray diffraction analysis. The iron state in the samples was controlled by the gamma resonance method.

A powder X-ray diffraction pattern of the $NaCuFe_2(VO_4)_3$ oxide was recorded at room temperature on a Bruker D8 ADVANCE diffractometer using a VANTEC linear detector (CuK_α radiation) at the Krasnoyarsk Territorial Center for Collective Use. A 2θ angle scanning step was 0.016° and an exposure time was 0.6 s per step.

Electron spin resonance (ESR) spectra in $NaCuFe_2(VO_4)_3$ were recorded on a Bruker Elexsys E580 spectrometer in the X band at temperatures of 110–300 K. The parameters used in recording the spectra were a microwave power of 0.63 mW, a modulation amplitude of 0.7 G, a modulation frequency of 100 kHz, a magnetic field sweep width of 5000 G, and a sweep time of 40 s.

Nuclear gamma resonance spectra were recorded at room temperature on powders with a thickness of 5–10 mg/cm^2 using of the natural iron content on an MS-1104Em spectrometer with a Co^{57}(Cr) source at the Kirensky Institute of Physics, Krasnoyarsk Scientific Center, Siberian Branch, Russian Academy of Sciences. The chemical shifts are presented relative to α-Fe.

The temperature dependence of specific heat was measured on a Quantum Design PPMS-6000 Physical Property Measurement System upon cooling the sample without magnetic field in the temperature range of 2–300 K and in magnetic fields of up to 9 T.

The static magnetic characteristics of the samples were measured in the zero field cooling (ZFC) and field cooling (FC) modes on an original SQUID magnetometer at the Kirensky Institute of Physics, Krasnoyarsk Scientific Center, Siberian Branch, Russian Academy of Sciences [16] in the temperature range of 4–300 K in a magnetic field of $H = 0.001$–0.05 T and on a Quantum Design MPMS-XL Magnetic Property Measurement System in the temperature range of 2–300 K in a magnetic field of 500 Oe.

3. RESULTS

Figure 1 shows a powder X-ray diffraction pattern of the $NaCuFe_2(VO_4)_3$ compound obtained at room temperature. According to the X-ray diffraction data, the synthesized samples are single-phase polycrystalline and the X-ray diffraction pattern contains no reflections corresponding to impurity phases. Since the structure of the $NaCuFe_2(VO_4)_3$ compound was previously resolved [11], it was used as an initial model for the Rietveld refinement in the HTOPAS 4.2 program [17]. Note that the refinement was stable and yielded low uncertainty factors (Table 1, Fig. 1). The atomic coordinates in the $NaCuFe_2(VO_4)_3$ crystal structure and the thermal parameters of the X-ray experiment are given in Table 2.

At room temperature, the $NaCuFe_2(VO_4)_3$ compound, similar to $LiCuFe_2(VO_4)_3$ [4, 11] is described by a triclinic symmetry space group P-1 with two formula units ($Z = 2$) per unit cell. Its charge composition is $Na^+Cu^{2+}Fe_2^{3+}(V^{5+}O_4)_3$. The synthesized

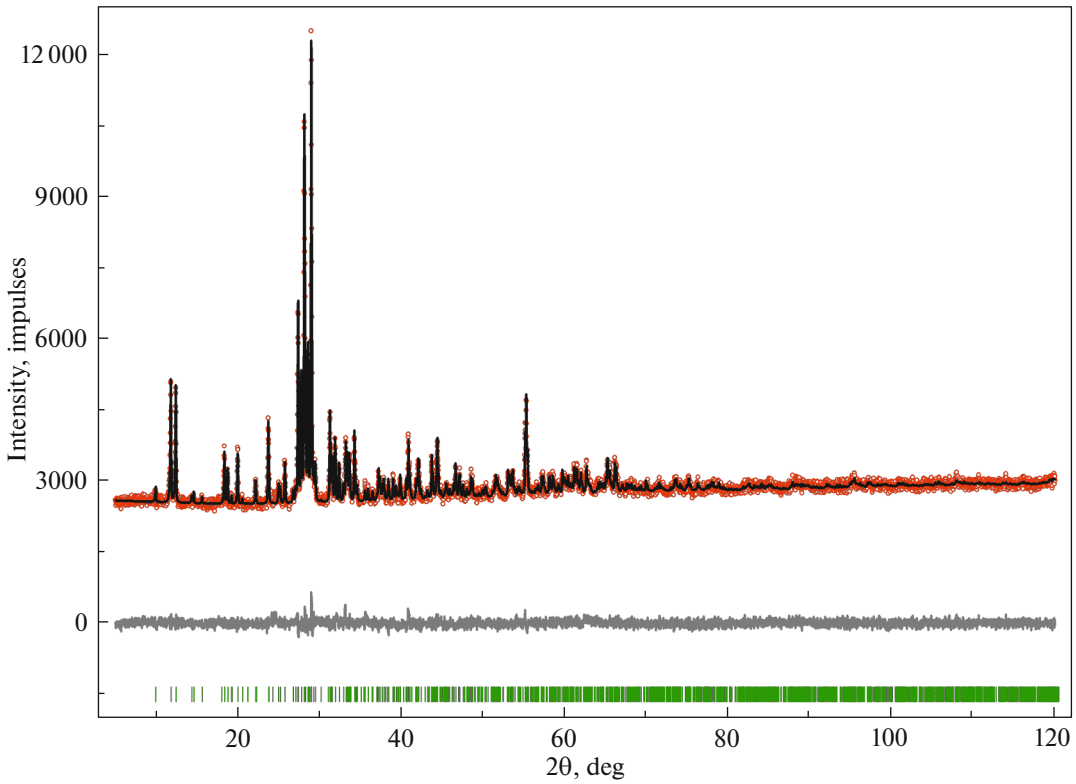

Fig. 1. X-ray diffraction patterns of the polycrystalline $NaCuFe_2(VO_4)_3$ compound at a temperature of $T = 300$ K.

$NaCuFe_2(VO_4)_3$ compound has the unit cell parameters (Table 1) similar to those of the natural howardevansite mineral [11], i.e., a = 8.198(2) Å, b = 9.773(1) Å, c = 6.6510(8) Å, α = 103.82(1)°, β = 101.99(1)°, γ = 106.74(1)°, and V = 473.1 Å^3.

The crystal structure of the complex isostructural $ACuFe_2(VO_4)_3$ (A = Na, Li) oxides consists of $Fe(1)O_6$ and $Fe(2)O_6$ iron octahedra; $V(1)O_4$, $V(2)O_4$, and $V(3)O_4$ vanadium tetrahedra; and trigonal CuO_5 bipyramids. Fe^{3+} ions occupy two crystallographically nonequivalent Fe(1) and Fe(2) sites in the unit cell. Two $Fe(1)O_6$ octahedra and two edge-sharing $Fe(2)O_6$ octahedra form dimeric structures. The dimers share edges with CuO_5 polyhedra and arrange in the chains extended along the b–c direction (Fig. 2). The dimers surrounded by VO_4 tetrahedra create the $Fe(1)_2V_8$ and $Fe(2)_2V_{10}$ formations arranged in a three-dimensional $[Fe_4V_6O_{24}]_\infty$ structure (frame). The frame voids are filled with A^+ ions (A = Na, Li). The face-sharing $A(1)O_6$ and $A(2)O_{10}$ formations are ordered in infinite zigzag chains extended along the b–c crystallographic direction. The features of the crystal structure of the $ACuFe_2(VO_4)_3$ system with magnetic $Fe^{3+}(1)$ and $Fe^{3+}(2)$ ions and Cu^{2+} ions give rise to the competing magnetic interactions with frustrations, which suggests the existence of a nontrivial spin configuration structure.

The ionic radii of univalent Na^+ ions and Li^+ ions are 0.98 and 0.68 Å, respectively [18]. The chemical pressure induced by the cationic substitution of sodium for lithium in $ACuFe_2(VO_4)_3$ changed, first, the lattice parameters (for $LiCuFe_2(VO_4)_3$, they are a = 8.1489(2) Å, b = 9.8047(2) Å, c = 6.6341(1) Å, α = 103.811(2)°, β = 102.370(2)°, γ = 106.975(2)°, and V = 468.74(2) Å^3 [4]) and, second, spacings between magnetic ions (Tables 1 and 3). It should be noted that these changes are anisotropic, which is indicated by an

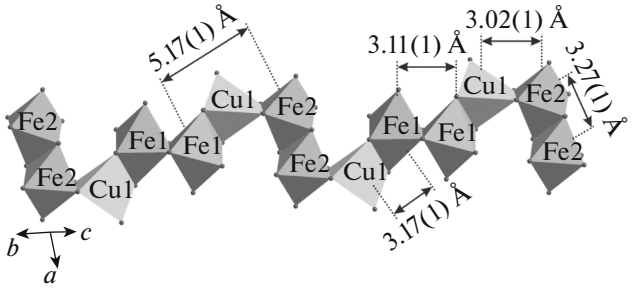

Fig. 2. Fragment of the crystal lattice. The chain of magnetic ions ...–$Fe^{3+}(2)$–$Fe^{3+}(2)$–Cu^{2+}–$Fe^{3+}(1)$–$Fe^{3+}(1)$–Cu^{2+}–$Fe^{3+}(2)$–$Fe^{3+}(2)$–... in the $NaCuFe_2(VO_4)_3$ structure with characteristic interatomic spacings.

Table 1. Main parameters of the X-ray diffraction experiment conducted at room temperature and results of refinement of the crystal structure of the $NaCuFe_2(VO_4)_3$ compound

Sp. gr.	$P-1$
a, Å	8.2063(2)
b, Å	9.7938(3)
c, Å	6.6581(2)
α, deg	103.855(2)
β, deg	102.042(2)
γ, deg	106.936(1)
V, Å^3	474.16(3)
2θ range	5–120
Number of reflections	1430
Number of refined parameters	94
R_{wp}, %	2.16
R_p, %	1.69
R_B, %	0.72
χ^2	1.17

a, b, c and α, β, γ are the cell parameters; V is the cell volume; R_{wp}, R_p, and R_B are the weight profile, profile, and integral weight parameters; and χ^2 is the fitting quality.

increase in the lattice parameters a, c, and V, a decrease in the parameter b, an increase in the spacings between magnetic ions $Fe^{3+}(1)$–$Cu(1)^{2+}$–$Fe^{3+}(2)$, $Fe^{3+}(2)$–$Fe^{3+}(2)$, and $Cu(1)^{2+}$–$Fe^{3+}(1)$, and a decrease in the spacings between magnetic ions $Fe^{3+}(1)$–$Fe^{3+}(1)$ and $Cu(1)^{2+}$–$Fe^{3+}(2)$.

It is well known that microscopic objects (crystallites and grain boundaries) inside bulk materials can significantly affect the properties of the latter. Using X-ray diffraction, we estimated the crystallite size in the $ACuFe_2(VO_4)_3$ (A = Na, Li) system. In the sodium-containing sample, the average crystallite size is 120(2) nm and, in combination with lithium, 83(1) nm. Thus, the grain size in these polycrystals depends on the chemical composition and holds a place at the upper boundary of nanoscale objects (~100 nm).

To characterize the $NaCuFe_2(VO_4)_3$ compound and elucidate the features caused by the chemical pressure induced by the cationic substitution of nonmagnetic ions, the electron spin resonance (ESR) study in the temperature range of 110–300 K was carried out. A single Lorentzian line was observed (Fig. 3a). The first derivative of the ESR absorption signal at room temperature has a linewidth of ΔH = 994 Oe and a g factor of g = 2.008. For comparison,

Table 2. Atomic coordinates, isotropic thermal parameters B_{iso} (Å^2), and occupancies of the crystal lattice sites of the $NaCuFe_2(VO_4)_3$ compound at a temperature of T = 300 K

	x	y	z	B_{ISO}	Occupancy
Cu1	0.7852(10)	0.7989(8)	0.7792(11)	1.0(3)	1
Fe1	0.5520(11)	0.3911(9)	0.1146(16)	0.2(3)	1
Fe2	0.2934(10)	0.9920(9)	0.4625(15)	0.2(2)	1
V1	0.4055(14)	0.6667(10)	0.3815(17)	2.0(3)	1
V2	0.8382(12)	0.7367(10)	0.2697(15)	1.9(3)	1
V3	0.7695(11)	0.1241(10)	0.0896(15)	0.6(3)	1
Na1	0	0.5	0.5	2.0(8)	1
Na2	0.004(7)	0.540(6)	−0.022(9)	2.0(11)	0.5
O1	0.430(3)	0.854(3)	0.425(4)	2	1
O2	0.482(4)	0.371(3)	0.376(6)	2	1
O3	0.815(3)	0.555(3)	0.285(4)	2	1
O4	0.228(4)	1.165(3)	0.501(5)	2	1
O5	0.301(4)	−0.002(3)	0.182(5)	2	1
O6	0.467(4)	0.586(3)	0.180(5)	2	1
O7	0.745(4)	0.750(3)	0.013(5)	2	1
O8	0.054(4)	0.826(3)	0.303(4)	2	1
O9	0.174(4)	0.573(4)	0.329(4)	2	1
O10	1.001(4)	0.249(3)	0.226(4)	2	1
O11	0.727(4)	0.037(4)	0.270(5)	2	1
O12	0.648(4)	0.244(4)	0.071(5)	2	1

Table 3. Distances between magnetic ions in the $NaCuFe_2(VO_4)_3$ and $LiCuFe_2(VO_4)_3$ compounds

Compound	$d_{Fe(1)-Fe(1)}$, Å	$d_{Fe(2)-Fe(2)}$, Å	$d_{Fe(1)-Cu(1)-Fe(2)}$, Å	$d_{Cu(1)-Fe(1)}$, Å	$d_{Cu(1)-Fe(2)}$, Å
$NaCuFe_2(VO_4)_3$	3.11(1)	3.27(1)	5.17(1)	3.17(1)	3.02(1)
$LiCuFe_2(VO_4)_3$	3.156(9)	3.112(7)	5.114(8)	3.121(8)	3.074(8)
Δd	−0.05	0.16	0.06	0.05	−0.05

$\Delta d = d_{NaCuFe_2(VO_4)_3} - d_{LiCuFe_2(VO_4)_3}$.

the results of investigations of the resonance characteristics of $LiCuFe_2(VO_4)_3$ [4] are presented (ΔH = 846 Oe and $g = 2.005$).

Figures 3b and 3d show the data on the temperature dependences of the magnetic resonance signal intensity (a product of the signal amplitude and the squared linewidth), width ΔH, and resonance field H_{res} of the observed ESR absorption derivative line for $NaCuFe_2(VO_4)_3$ and $LiCuFe_2(VO_4)_3$. It can be seen that, for both samples, the resonance field in the tem-

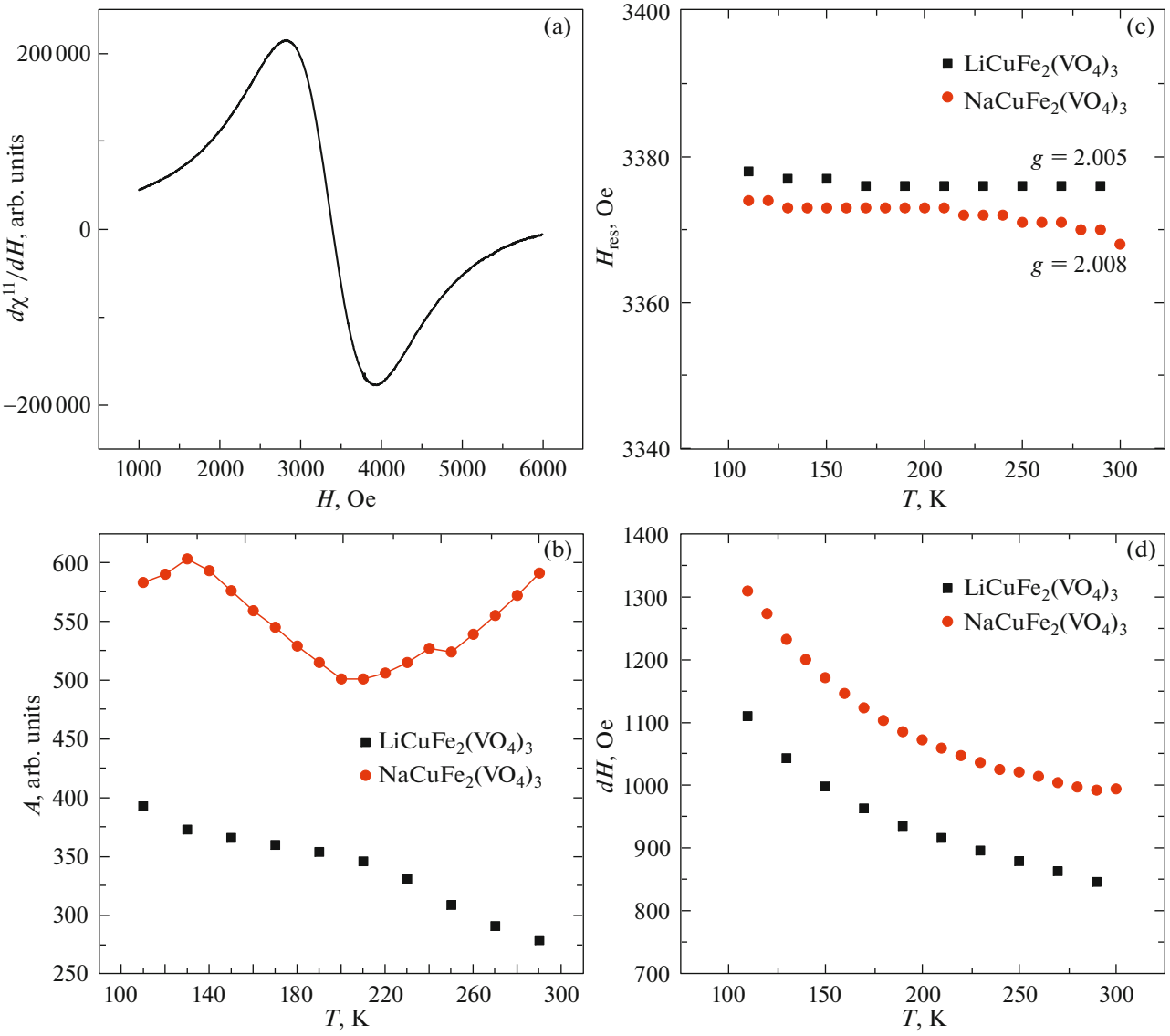

Fig. 3. (a) Room-temperature ESR spectrum of the $NaCuFe_2(VO_4)_3$ compound in the X band. Temperature dependences of (b) the amplitude, (c) resonance field, and (d) linewidth of the ESR signal for the $NaCuFe_2(VO_4)_3$ and $LiCuFe_2(VO_4)_3$ samples.

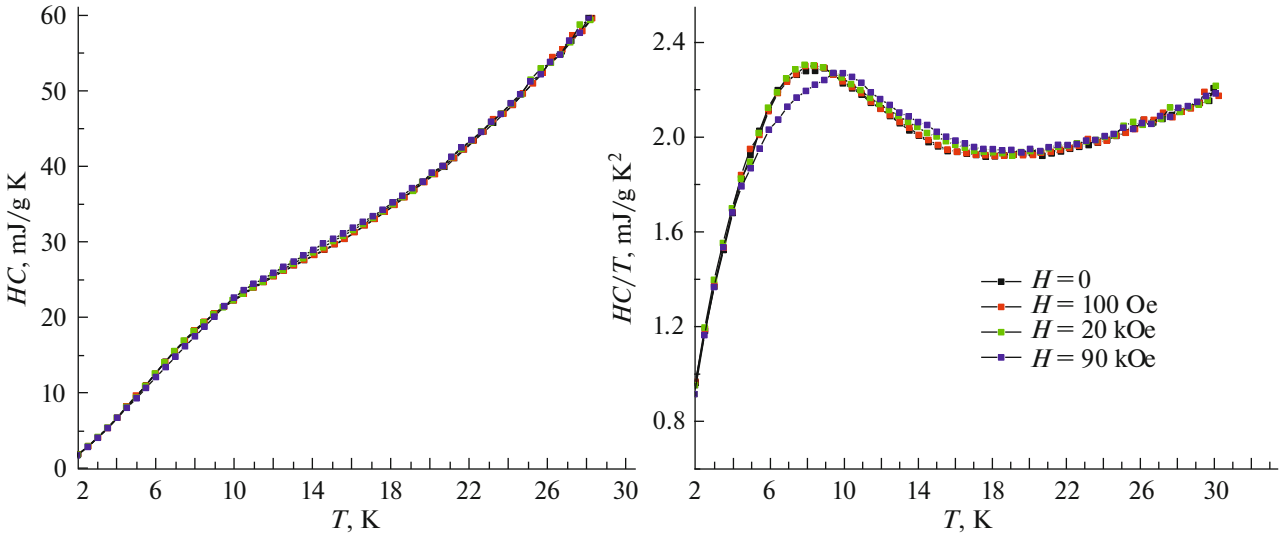

Fig. 4. Temperature dependences of specific heat HC (on the left) and HC/T (on the right) at magnetic fields of $H = 0$, 100 Oe, 20 kOe, and 90 kOe for $NaCuFe_2(VO_4)_3$. The sample mass is $m = 21.42$ mg.

perature range of 110–300 K remains almost unchanged (Fig. 3c). As the temperature decreases, the linewidth ΔH monotonically increases, which is related to both an increase in the local field spread on magnetic ions and an increase in the relaxation time. In this case, the ΔH value for $LiCuFe_2(VO_4)_3$ is lower than for $NaCuFe_2(VO_4)_3$ by approximately 15% over the entire investigated temperature range. This can be caused by the chemical pressure induced by the replacement of one univalent element (Li) by another (Na), which leads to a significant increase in the interionic spacing Fe(2)–Fe(2) (Table 3) and, consequently, a decrease in the exchange coupling between the ions.

The thermal properties of the $NaCuFe_2(VO_4)_3$ powder sample were studied in the temperature range of 2–300 K in magnetic fields of up to 90 kOe. Figure 4 shows temperature dependences of specific heat HC (on the left) and HC/T values (on the right) in magnetic fields of $H = 0$, 100 Oe, 20 kOe, and 90 kOe. It was found that the temperature dependence of HC/T for $NaCuFe_2(VO_4)_3$ is anomalous. In zero magnetic field, the maximum of the broad anomaly in the $HC(T)/T$ curve observed at a temperature of $T \approx 8.5$ K is indicative of the phase transformation in the sample. An applied dc magnetic field of up to $H =$ 20 kOe does not qualitatively change the temperature dependence of specific heat; in stronger fields, however, the $HC(T)/T$ maximum shifts toward higher temperatures (Fig. 4, $H = 90$ kOe, the temperature shift is $\Delta T \approx T_{H = 90\ \text{kOe}} - T_{H = 0} = 1$–1.5 K). This is most likely due to the features of the response of the $NaCuFe_2(VO_4)_3$ magnetic subsystem to the external magnetic field; possibly, spin formations inside crystallites coarse and the spin structure of the intergrain layer changes.

The measured magnetic characteristics of $NaCuFe_2(VO_4)_3$ presented in Fig. 5 reveal a nontrivial behavior of the magnetic subsystem.

The temperature dependence of the inverse static magnetic susceptibility $1/\chi(T)$ measured in a magnetic field of $H = 500$ Oe (a sample mass of $m = 0.015$ g) is shown in Fig. 5a. According to the experimental data, the $NaCuFe_2(VO_4)_3$ susceptibility at high temperatures ($T > 75$ K) obeys the Curie–Weiss law with a Curie–Weiss constant of $C = 0.016$ K and an asymptotic Néel temperature of $\theta = -75$ K, which is indicative of the dominance of antiferromagnetic exchange interactions in the paramagnetic region. At high temperatures, the $NaCuFe_2(VO_4)_3$ paramagnet has an effective magnetic moment of $\mu_{\text{eff(calc)}} = 8.4\mu_B$ per formula unit, which almost coincides with a calculated value of $\mu_{\text{eff(calc)}} = 8.5\mu_B$ ($\mu^{Fe^{3+}}_{\text{eff(calc)}} = 5.91\mu_B$ and $\mu^{Cu2}_{\text{eff(calc)}} = 1.73\mu_B$). The estimation of the magnetic frustrations f in $NaCuFe_2(VO_4)_3$ by the ratio $f = |\theta|/T_N$, yields a fairly high value of $f = 9.4$ (a typical value for a nonfrustrated antiferromagnet is $f = 2$–4.5 [19]).

Figure 5b shows the temperature dependence of the magnetic moment $M(T)$ for $NaCuFe_2(VO_4)_3$ measured on the sample with a mass of $m = 0.165$ g in a magnetic field of $H = 500$ Oe under different sample cooling conditions (zero field cooling (ZFC) and field cooling (FC) at $H = 500$ Oe). It can be seen that the temperature dependence of the magnetic moment in the low-temperature region is anomalous and, at temperatures below the irreversibility temperature $T_n \approx$ 3.5 K, it depends on the magnetic prehistory of the sample. Upon cooling in the ZFC mode, the magnetic

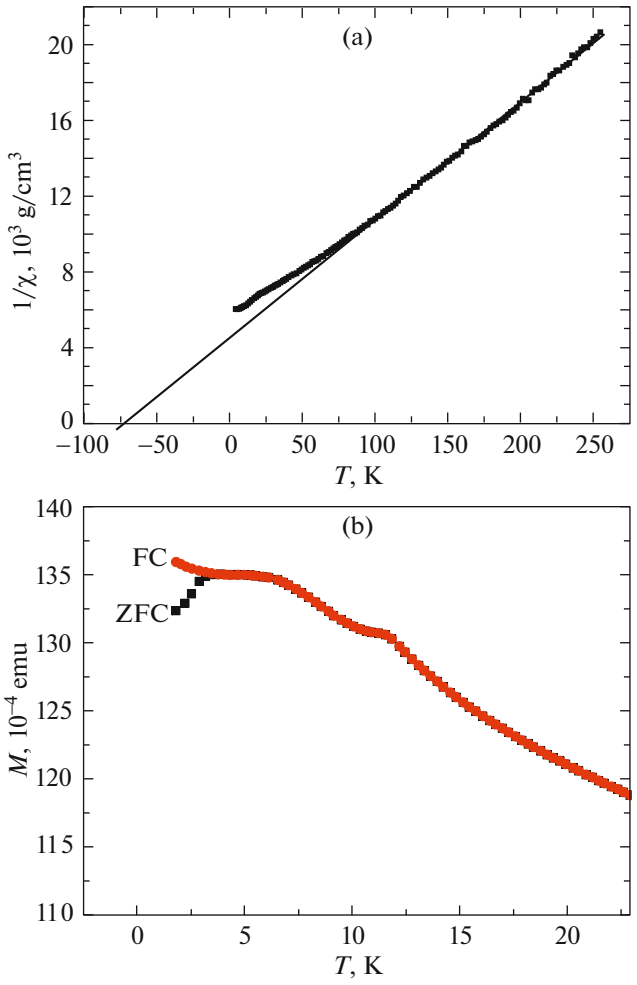

Fig. 5. (a) Temperature dependence of the inverse magnetic susceptibility of the $NaCuFe_2(VO_4)_3$ compound in a magnetic field of $H = 500$ Oe. The sample mass is $m = 0.015$ g. (b) Temperature dependence of the magnetic moment of $NaCuFe_2(VO_4)_3$ in a magnetic field of $H = 500$ Oe in the zero field cooling (ZFC) mode and in a magnetic field of $H = 500$ Oe (FC). The sample mass is $m = 0.165$ g.

moment increases with temperature, attains a broad maximum at $T_{max} \sim 5$ K, and then decreases. One of the main causes for this broad maximum in the ZFC temperature dependence of the magnetic moment can be the low dimensionality of the magnetic subsystem.

Upon cooling the sample in the FC mode at low temperatures, the magnetic moment decreases with an increase in temperature to ~3.5 K; during the further temperature growth, the ZFC and FC curves completely coincide. It is well known that the difference between the magnetic moments M(FC) and M(ZFC) is observed in systems of magnetic nanoparticles [20, 21] and macroscopic magnets with disordered elements (frustration of exchange bonds, topological disorder, and structural defects) [19, 20]. Note that the discrepancy between the ZFC and FC temperature dependences of the magnetic moment (Fig. 5b) for $NaCuFe_2(VO_4)_3$ was not found in the lithium-containing compound [2, 4]. Apparently, the enhancement of the heterogeneity, which can be caused by the occurrence of additional defects in the samples containing a coarser sodium ion, leads to disordered magnetism. We return to this question below when discussing the gamma resonance data on the samples.

As the temperature increases, in the vicinity of $T \sim 11$ K, another feature arises in the temperature dependence of the magnetic moment $M(T)$ of $NaCuFe_2(VO_4)_3$. The presence of two anomalies in the $M(T)$ curve is consistent with the results reported in [2]. The anomaly near 11 K is caused by the long-range magnetic order forming in the multisublattice $NaCuFe_2(VO_4)_3$ magnet. Under the action of temperature, above the Néel temperature $T_N \sim 11$ K, the spontaneous ordering in the sublattices is violated, which is accompanied by the occurrence of an anomaly not only in the temperature dependence of the magnetic moment, but also in the temperature dependence of specific heat (Fig. 4). It is worth noting that the Néel temperatures determined from the maximum in the dependences of the magnetic susceptibility ($T_N \approx 11$ K) and the $HC(T)/T$ value ($T_N \approx 8.5$ K) and corresponding to the phase transition from the ordered magnetic state to the paramagnetic phase are different, which can be related to blurring of the anomalies in the physical properties due to the nonuniform distribution of iron atoms over the nonequivalent crystallographic positions. This assumption is consistent with the results of investigations of the anomalous physical properties in the region of phase transitions in a medium with a nonuniform distribution of cations [22].

To refine the structural features and determine the nonequivalent sites, valence state, and coordination environment of iron ions in the $NaCuFe_2(VO_4)_3$ and $LiCuFe_2(VO_4)_3$ compounds, we carried out the gamma resonance study on ^{57}Fe nuclei. The room-temperature $NaCuFe_2(VO_4)_3$ and $LiCuFe_2(VO_4)_3$ Mössbauer spectra are shown in Fig. 6 (on the left). The spectra of the samples in the paramagnetic temperature range are sums of several quadrupole doublets. To identify the nonequivalent sites and iron states, we determined the quadrupole splitting distribution $P(QS)$ in the experimental spectra. To do that, a sum of two groups of seed doublets with different chemical shifts and natural linewidths was fitted to the experimental spectrum. Two values of the chemical shift characterizing two groups of doublets and the doublet line amplitudes were varied. The $P(QS)$ distributions obtained by this fitting are shown in Fig. 6 (on the right). The $P(QS)$ peaks and features indicate possible nonequivalent iron sites in these materials. Figure 6 (on the right) shows the chemical shifts for two groups of doublets obtained by the fitting. The data

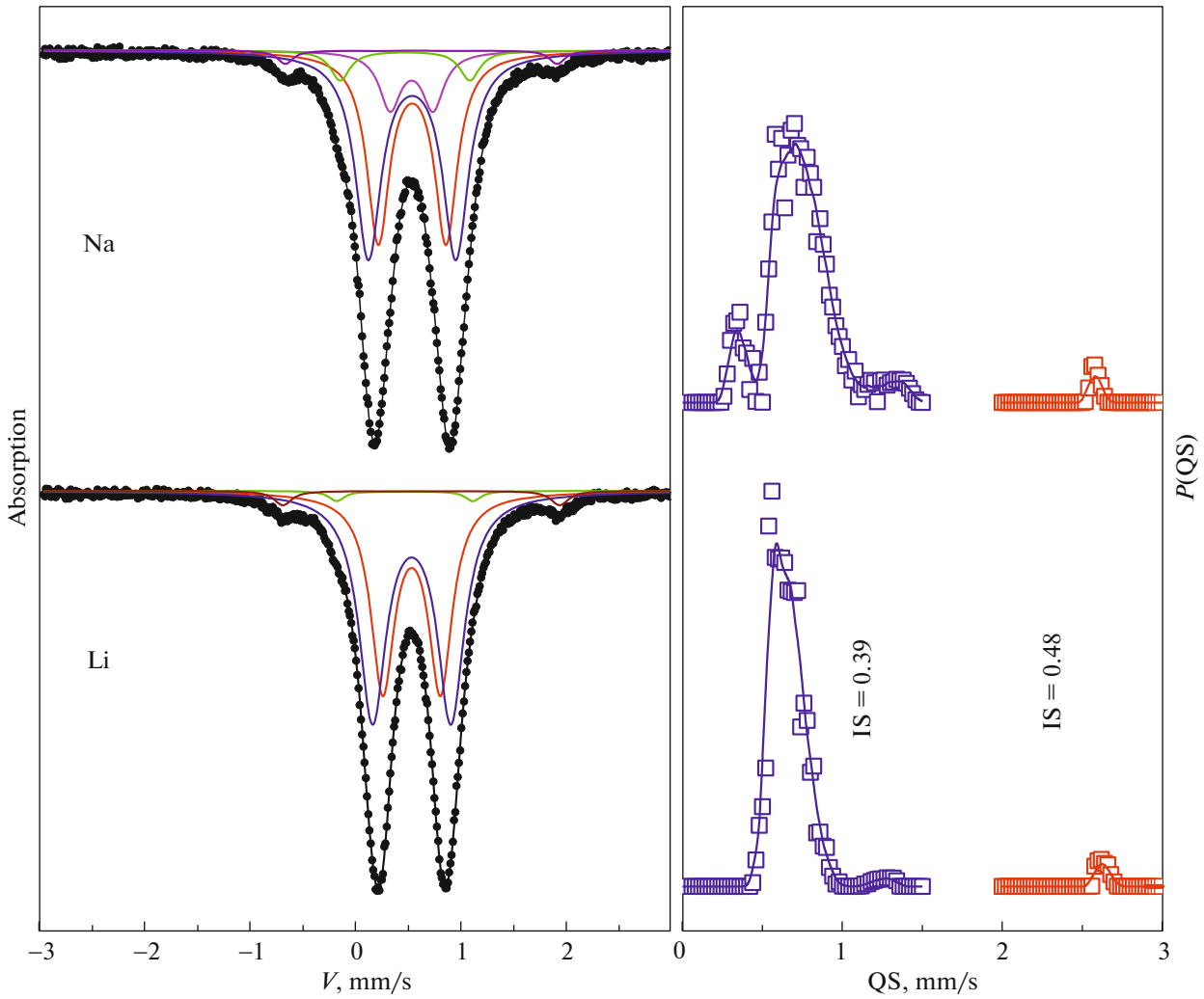

Fig. 6. Mössbauer spectra of the $NaCuFe_2(VO_4)_3$ and $LiCuFe_2(VO_4)_3$ compounds at a temperature of $T = 300$ K (on the left; the color lines show the spectrum components with the parameters given in Table 4) and probabilities of the quadrupole splittings for two chemical shifts (on the right).

obtained from the $P(QS)$ distributions were used to build model spectra fitted to the experimental ones by varying all the hyperfine structure parameters. The fitting results are given in Table 4.

An analysis of the experimental spectra shows that iron contained in $NaCuFe_2(VO_4)_3$ and $LiCuFe_2(VO_4)_3$ is in the trivalent high-spin ($S = 5/2$) state and octahedral oxygen environment.

The result of identification of the $LiCuFe_2(VO_4)_3$ spectrum shows that this compound contains four nonequivalent iron sites. Two of them have high relative occupancies (41% and 55%). The two remaining sites have a minimum occupancy (2%) comparable with the experimental error. Nevertheless, they are clearly seen in the Mössbauer spectra and in the $P(QS)$ distribution (Fig. 6). For crystallographic binding of the nonequivalent iron sites, we used the proportionality of quadrupole splitting to the electric field gradient. For this purpose, we calculated the main component of the gradient $|V_{zz}|$ induced by the coordination oxygen polyhedron surrounding the cations in the $LiCuFe_2(VO_4)_3$ structure using the X-ray data on the atomic coordinates in this material. In column Site of Table 4, the identified crystallographic sites are given in accordance with the correlation $QS \sim V_{zz}$. Analyzing the relative occupancies of the iron sites, we can clearly see that iron cations that left the Fe1 crystallographic sites entered the Cu and Li ones.

In $NaCuFe_2(VO_4)_3$, we found five nonequivalent iron sites. Analyzing the correlation of the quadrupole splitting and electric field gradient for different crystallographic sites, we may conclude with a high degree of probability that Na cations lead to the splitting of the Fe1crystallographic sites into two Fe1' and Fe1" sites with different degrees of distortion. The ratio between occupancies of these sites are 1 : 4. The X-ray

Table 4. Room-temperature Mössbauer parameters of $NaCuFe_2(VO_4)_3$ and $LiCuFe_2(VO_4)_3$ compounds

	IS, mm/s ±0.005	QS, mm/s ±0.01	W, mm/s ±0.01	A, frac.% ±0.03	$\lvert V_{zz}\rvert$, e/Å^3	Site	$\langle r\rangle$, Å
Li	0.380	0.55	0.27	0.41	0.186	Fe1(6)	2.058
	0.381	0.75	0.31	0.55	0.214	Fe2(6)	1.989
	0.315	1.29	0.18	0.02	0.438	Li1(6)	2.230
	0.472	2.63	0.20	0.02	0.565	Cu(5)	2.030
Na	0.380	0.41	0.25	0.11	0.200	Fe1'(6)	2.074
	0.385	0.64	0.26	0.37		Fe1"(6)	
	0.385	0.83	0.29	0.45	0.191	Fe2(6)	1.982
	0.317	1.23	0.22	0.05	0.335	Na1(6)	2.303
	0.471	2.58	0.18	0.02	0.592	Cu(5)	2.035

IS is the isomeric shift relative to α-Fe, QS is the quadrupole splitting, W is the absorption linewidth, A is the fractional occupancy of the site with iron, V_{zz} is the electric field gradient, and $\langle r\rangle$ is the mean interionic spacing in the coordination polyhedron.

diffraction technique did not allow us to reliably separate these contributions because of the random distribution of sites over the crystal, so only averaged coordinates were obtained for the Fe1 crystallographic sublattice. In $NaCuFe_2(VO_4)_3$, iron atoms migrate also to foreign sites, but, in contrast to the Li sample, it mainly occurs from the Fe2 to Na1 sites. In addition, the substitution of Na for Li is accompanied by an increase in the interionic distances in the Na1(6) polyhedron and, to a lesser extent, in the Fe1(6) polyhedron.

Thus, analyzing the Mössbauer data obtained on the $ACuFe_2(VO_4)_3$ system, we can see that it is important, in the context of this study, that additional iron sites arise in $NaCuFe_2(VO_4)_3$, unlike the case of $LiCuFe_2(VO_4)_3$; i.e., the disorder in the iron cation distribution in the sodium-containing sampler is greater.

In $NaCuFe_2(VO_4)_3$, Fe^{3+} ions ($3d^5$ electronic configuration, spin $S = 5/2$) and Cu^{2+} ions ($3d^9$ electronic configuration, spin $S = 1/2$) are responsible for magnetism. The coexistence of $Fe^{3+}(1)$ and $Fe^{3+}(2)$ iron located in two nonequivalent crystallographic sites and forming the structural elements dimers, splitting of the Fe1 crystallographic sites into Fe1' and Fe1" sites with different degrees of distortion, and $Cu^{2+}(1)$ ions occupying a single crystallographic site in the magnetic subsystem of the investigated iron oxide compound leads to the competition of the exchange interactions, which affect the orientation of spins in the ordered state. In addition, a feature of the $NaCuFe_2(VO_4)_3$ magnetic subsystem, as in $LiCuFe_2(VO_4)_3$, is that the chains with magnetically active ions are separated by the nonmagnetic VO_4 formations; as a result, according to the estimates of the exchange interactions from [2, 4], the interchain exchange interaction is weaker than the exchange inside a chain.

The exchange interaction in the chains of magnetic ions of the $ACuFe_2(VO_4)_3$ (A = Na, Li) system, which is implemented via the superexchange between the nearest magnetic moments, depends on the spacings between them and the exchange coupling angles. The crystal structure violations caused by the incorporation of a coarser sodium ion instead of lithium not only change the ratio between the antiferromagnetic and ferromagnetic contributions to the total exchange interaction, but also to the break of periodicity of their changes, leading to the disordered magnetism in $NaCuFe_2(VO_4)_3$ at low temperatures.

The features of the topology of the exchange interactions and their competition apparently facilitate the formation of a nontrivial spin architecture in the temperature range with the long-range magnetic order of the frustrated $ACuFe_2(VO_4)_3$ (A = Na, Li) system. As is known, the only direct method for determining the magnetic structure of compounds is magnetic neutron diffraction. At present, there has been a lack of data on magnetic structures and transitions between them in the $ACuFe_2(VO_4)_3$ system. We attempted to conduct experiments on the scattering of neutrons with a wavelength of $\lambda = 1.488$ Å in the low-temperature (from 1.5 K) range on a WAND diffractometer at the Oak Ridge National Laboratory (USA). Unfortunately, the study of the $NaCuFe_2(VO_4)_3$ and $LiCuFe_2(VO_4)_3$ magnets by elastic neutron scattering did not allow us to establish the magnetic ordering type.

4. CONCLUSIONS

The $NaCuFe_2(VO_4)_3$ compound was synthesized by the solid-state reaction and its structural, resonant,

thermal, and static magnetic properties were examined. A comparison of the properties of the $ACuFe_2(VO_4)_3$ (A = Na, Li) compounds allowed us to identify the characteristic features of the sodium-containing sample and establish the effect of chemical pressure induced by the cationic substitution of sodium atoms for lithium ones.

According to the X-ray diffraction data, at room temperature, the $NaCuFe_2(VO_4)_3$ polyvanadate is characterized by a triclinic symmetry space group $P-1$. The chemical pressure induced by the substitution of sodium for lithium in the $ACuFe_2(VO_4)_3$ system does not violate the crystal lattice symmetry, but leads to the anisotropic change in the crystal lattice parameters and spacings between magnetically active ions forming chains separated from each other and affects the crystallite size.

The Mössbauer data on the samples showed that iron in $ACuFe_2(VO_4)_3$ is in the trivalent high-spin ($S = 5/2$) state and octahedral oxygen environment. The refinement of the structural features showed that a significant difference between the lithium and sodium ionic radii enhances the distortion of the oxygen octahedron around the iron cation in $NaCuFe_2(VO_4)_3$ as compared to $LiCuFe_2(VO_4)_3$ and causes the separation of the Fe1 crystallographic site into two sites with different degrees of distortion of the local environment, leading to an increase in the number of nonequivalent iron sites. In addition, the noticeable migration of iron from the Fe2(6) to Na1(6) sites in $NaCuFe_2(VO_4)_3$ was found. Thus, the real crystal structure of $NaCuFe_2(VO_4)_3$ seems to be weaker ordered than the $LiCuFe_2(VO_4)_3$ structure.

In addition, it was found that, in the temperature range of 110–300 K, the characteristic ESR parameters of the spectra of the lithium- and sodium-containing samples have similar temperature dependences. The g factors close to 2 for both compounds indicate that the main contribution to the magnetic resonance signal is made by trivalent S iron ions. An increase in the magnetic resonance linewidth was found in the samples containing sodium ions as compared with the lithium-containing samples, which is apparently caused by a decrease in the exchange interaction between Fe(2)–Fe(2) ions due to a significant change in the spacing between them and occurrence of additional nonequivalent positions of the Fe1' and Fe1" iron ions with different degrees of distortion of the oxygen environment.

In the $NaCuFe_2(VO_4)_3$ magnet with the exchange interaction strong inside the chains and weak between them at low temperatures, the competition of the exchange interactions with different signs and values leads to the frustrated magnetic state, which is one of the reasons for the complex behavior of the magnetic subsystem. We observed a nonmonotonic displacement of the anomaly in the temperature dependence of specific heat of $NaCuFe_2(VO_4)_3$, which is responsible for the formation of a long-range magnetic order, toward high temperatures in an external magnetic field. The discrepancy in the ZFC and FC temperature dependences of the magnetic moment at temperatures below 3.5 K in $NaCuFe_2(VO_4)_3$ is related to the nonuniform distribution of iron cations over the nonequivalent crystallographic sites found by the X-ray and, in more detail, gamma-resonance studies.

The results of the study demonstrate the effect of the cationic substitution on the physical properties and the possibility of controlling them by changing the chemical pressure in multicomponent vanadates with the general formula $ACuFe_2(VO_4)_3$.

ACKNOWLEDGMENTS

The authors are grateful to the authorities of the Oak Ridge National Laboratory (USA) for presenting the opportunity of conducting neutron diffraction experiments and Matthias D. Frontzek for performing the measurements.

CONFLICT OF INTEREST

The authors declare that they have no conflicts of interest.

REFERENCES

1. N. Guskos, G. Zolnierkiewicz, J. Typek, R. Szymczak, A. Guskos, P. Berczynski, and A. Blonska-Tabero, Mater. Sci. Poland **31**, 601 (2013).
2. A. V. Koshelev, K. V. Zakharov, L. V. Shvanskaya, A. A. Shakin, D. A. Chareev, S. Kamusella, H.-H. Klauss, K. Molla, B. Rahaman, T. Saha-Dasgupta, A. P. Pyatakov, O. S. Volkova, and A. N. Vasiliev, Phys. Rev. Appl. **10**, 034008 (2018).
3. M. A. Lafontaine, J. M. Grenéche, Y. Laligant, and G. Férey, J. Solid State Chem. **108**, 1 (1994).
4. T. V. Drokina, G. A. Petrakovskii, O. A. Bayukov, A. M. Vorotynov, D. A. Velikanov, and M. S. Molokeev, Phys. Solid State **58**, 1981 (2016).
5. Yu. A. Izyumov, *Neutron Diffraction on Long-Period Structures* (Energoatomizdat, Moscow, 1987) [in Russian].
6. S. S. Sosin, L. A. Prozorova, and A. I. Smirnov, Phys. Usp. **48**, 83 (2005).
7. R. S. Gekht, Sov. Phys. JETP **75**, 1058 (1992).
8. A. K. Murtazaev, M. K. Ramazanov, and M. K. Badiev, Phys. Solid State **52**, 1673 (2010).
9. R. S. Gekht and I. N. Bondarenko, J. Exp. Theor. Phys. **86**, 1209 (1998).
10. R. S. Gekht and I. N. Bondarenko, J. Exp. Theor. Phys. **84**, 345 (1997).
11. J. M. Hughes, J. W. Drexler, C. F. Campana, and M. L. Malinconico, Am. Mineralog. **73**, 181 (1988).
12. A. A. Belik, Mater. Res. Bull. **34**, 1973 (1999).

13. T. V. Drokina, G. A. Petrakovskii, A. L. Freidman, M. S. Molokeev, and E. G. Rezina, RF Patent No. 2592867 (2016).
14. S. Kamoun, F. Hlel, and M. Gargouri, Ionics **20**, 1103 (2014).
15. S. Kamoun and M. Gargouri, Ionics **21**, 765 (2014).
16. D. A. Velikanov, Vestn. SibGAU **2**, 176 (2013).
17. *Bruker AXS TOPAS V4: General Profile and Structure Analysis Software for Powder Diffraction Data, User's Manual* (Bruker AXS, Karlsruhe, Germany, 2008).
18. N. S. Akhmetov, *General and Inorganic Chemistry* (Vysshaya Shkola, Akademiya, Moscow, 2001).
19. J. A. Mydosh, *Spin-Glasses: An Experimental Introduction* (Taylor and Francis, New York, 1993).
20. S. P. Gubin, Yu. A. Koksharov, G. B. Khomutov, and G. Yu. Yurkov, Russ. Chem. Rev. **74**, 489 (2005).
21. N. V. Mushnikov, *Magnetism and Magnetic Transitions* (UrFU, Yekaterinburg, 2017) [in Russian].
22. E. A. Mikhaleva, I. N. Flerov, V. S. Bondarev, M. V. Gorev, A. D. Vasil'ev, and T. N. Davydova, Phys. Solid State **53**, 510 (2011).

Translated by E. Bondareva